

# 3D element-to-tissue correlation determined by continuous confocal $\mu$ -XRF scanning at Beamline L

<sup>1</sup>B. De Samber, <sup>2</sup>R. Evens, <sup>2</sup>K. De Schamphelaere, <sup>2</sup>C. Janssen, <sup>3</sup>B. Masschaele,  
<sup>3</sup>L. Van Hoorebeke, <sup>1</sup>B. Vekemans, <sup>4</sup>G. Falkenberg, <sup>4</sup>K. Rickers, I. Szaloki and <sup>1</sup>L. Vincze

<sup>1</sup>X-ray Microspectroscopy and Imaging (XMI), Ghent University, Krijgslaan 281, Ghent, Belgium

<sup>2</sup>Laboratory of Environmental Toxicology and Aquatic Ecology, Jozef Plateaustraat 22, Ghent, Belgium

<sup>3</sup>Centre for X-Ray Tomography, Department of Subatomic and Radiation Physics, Ghent, Belgium

<sup>4</sup>Hamburger Synchrotronstrahlungslabor at DESY, Notkestr. 85, D-22603 Hamburg, Germany

Confocal micro-XRF is a relatively new local analysis method which allows to analyse the trace level metal contents within the confocal volume formed by the coinciding foci of the excitation and detection side polycapillary [1]. When using a scanning algorithm, virtual sections of elemental distributions can be obtained without the need of rotating the sample. Combined with a dynamic scanning algorithm [2], a considerable reduction in measuring time can be achieved for measuring a single virtual slice through the sample, thus allowing to measure a series of subsequent slices. This makes it possible to deliver a three dimensional image of the trace level metal distributions inside the sample.

As a case study, a 3D confocal analysis was performed on a single egg (ca. 300  $\mu\text{m}$  diameter) of *Daphnia magna*, a frequently used model organism to investigate the influence of heavy metals. In Fig. 1, 2D confocal micro-XRF scanning results show the elemental distributions of Ca, Fe, Zn and Compton scattering of a single plane through the sample. The dynamic scanning algorithm was adapted with a third motor, making it possible to measure a total amount of 16 planes (59 x 67 pixels, 5  $\mu\text{m}$  step size), each 10  $\mu\text{m}$  away from each other. This resulted in a total amount of 63248 single XRF spectra and a total measuring time of  $\sim$ 18h. Data processing was performed by the AXIL software using symmetric multiprocessing (SMP) on a quad core server system. In Fig. 2 (left) 16 confocal element slices of Fe are shown which clearly reveal the depth dependent presence of different cavities. In Fig. 2 (right), an Fe isosurface was rendered under different viewing angles using the Xvolume applet within the IDL software. The isosurface clearly reveals the presence of 4 different cavities in a more clear manner, thus facilitating the interpretation of the measured dataset.

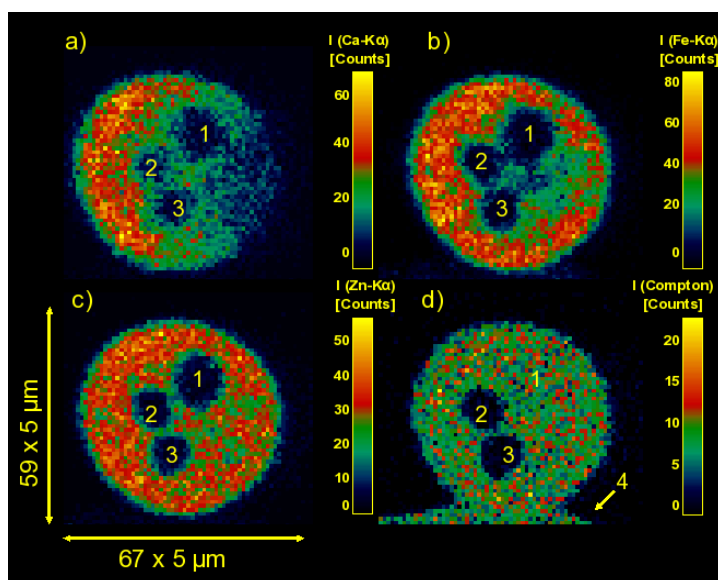


Figure 1: Ca, Fe and Zn element distributions through a single egg of *D. magna*

In Fig 3a) to 3c), isosurfaces of the Fe, Zn elemental distributions and Compton scattering were rendered. In order to verify the coinciding presence of elements, a combined RGB image of the isosurfaces is shown in Fig. 3d). The yellow areas indicate internal spheres with a similar density as the bulk of the sample, but lacking the presence of Fe and Zn. The white areas show the interface between the bulk of the sample and the air. In a previous contribution, we showed that when a sample is also analysed using laboratory  $\mu$ -CT it is possible to couple the 2D element information to the 3D internal structure/morphology of the sample [3]. With a 3D confocal dataset, it is possible to obtain a full element-to-tissue correlation in all scanning dimensions, providing more information on the sample of interest (Fig. 3d and 3e).

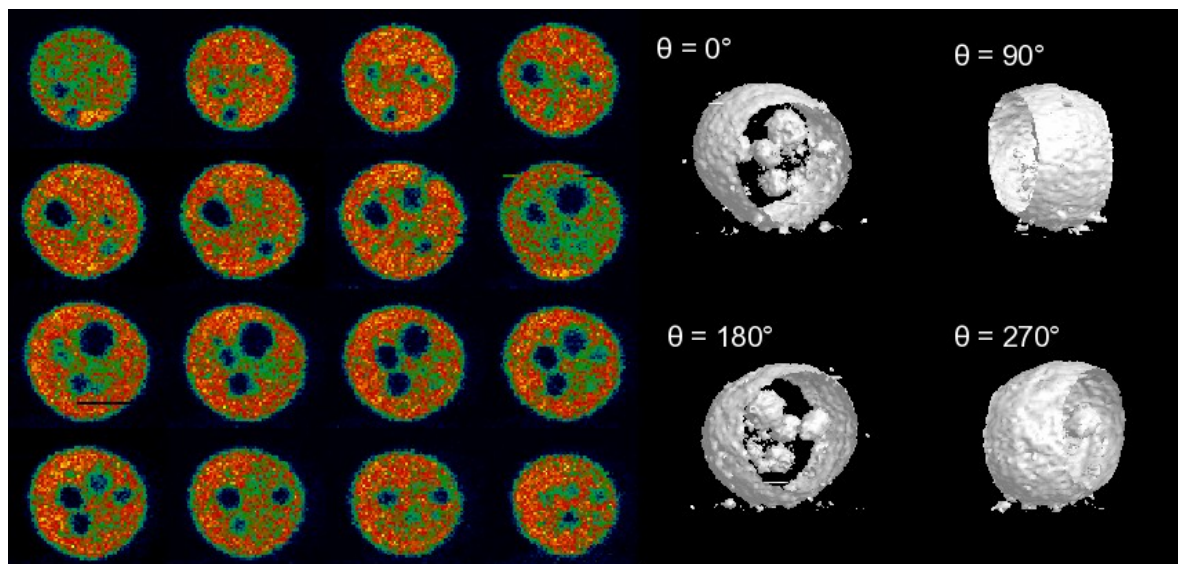


Figure 2: 16 subsequent depth distributions of Fe through an egg of *Daphnia magna* (left), Fe isosurface rendered under 4 different rotation angles (right)

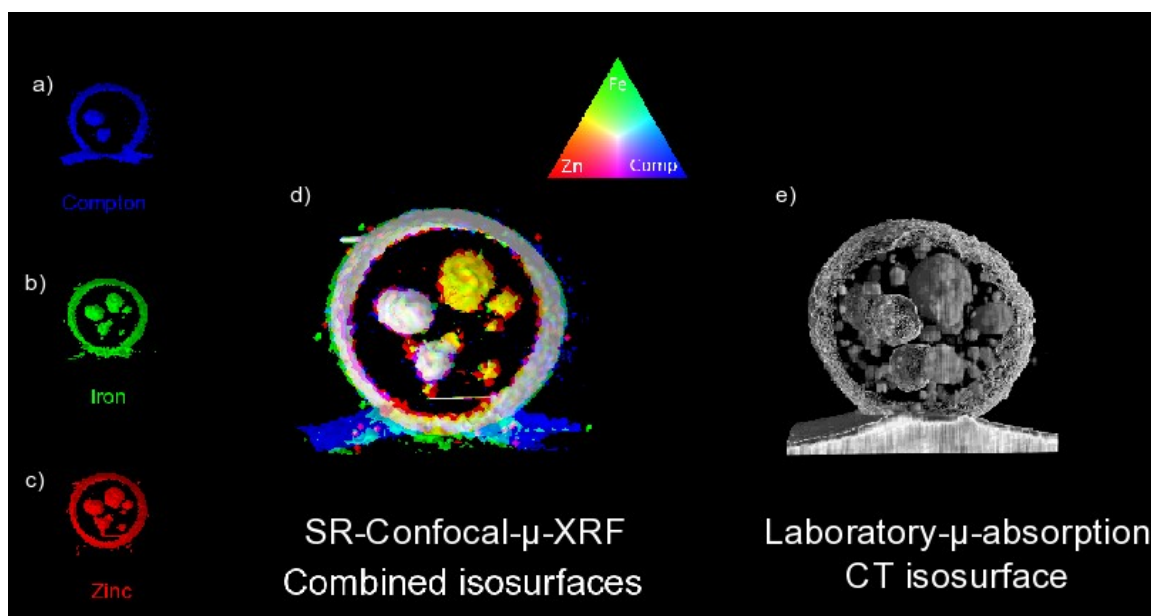


Figure 3: a) to c) isosurfaces of Fe, Zn and Compton scattering of a single *Daphnia magna* egg. d) RGB combined isosurfaces e) laboratory micro absorption CT isosurface

## References:

- [1] L. Vincze et al., *Analytical Chemistry*, **76**, 6786-6791 (2004)
- [2] G. Falkenberg et al., *Hasylab Annual Report*, 91-95 (2005)
- [3] De Samber et al., *Hasylab Annual Report*, 1281-1282 (2007)